Journal of Photochemistry and Photobiology A: Chemistry 204 (2009) 168–173

Contents lists available at ScienceDirect

Journal of Photochemistry and Photobiology A: Chemistry

journal homepage: www.elsevier.com/locate/jphotochem

Photosensitization of TiO_2 by Ag_2S and its catalytic activity on phenol photodegradation

M.C. Neves[a], J.M.F. Nogueira[b], T. Trindade[a], M.H. Mendonça[c], M.I. Pereira[c], O.C. Monteiro[b,*]

[a] University of Aveiro, Department of Chemistry, CICECO, 3810-193 Aveiro, Portugal
[b] University of Lisbon, Faculty of Sciences, Department of Chemistry and Biochemistry, CQB, Campo Grande, 1749-016 Lisbon, Portugal
[c] University of Lisbon, Faculty of Sciences, Department of Chemistry and Biochemistry, CCMM, Campo Grande, 1749-016 Lisbon, Portugal

ARTICLE INFO

Article history:
Received 27 November 2008
Received in revised form 18 March 2009
Accepted 21 March 2009
Available online 31 March 2009

Keywords:
Phenol
Photodegradation
TiO_2/Ag_2S
Photocatalysis
Photosensitizer

ABSTRACT

A process of TiO_2 photosensitization by coupling it with a narrow band gap semiconductor has been investigated here. Distinct TiO_2/Ag_2S nanocomposites were prepared by a single-source decomposition method. After sensitization, the TiO_2 materials were evaluated as photocatalysts on the degradation of aqueous phenol solutions. The experimental results show that the nanocomposites photocatalytic activity is related with the existence of Ag_2S over the TiO_2 surface. The best catalytic results, for phenol photodegradation, were obtained using a TiO_2/Ag_2S material with a surface Ti/Ag atomic ratio equal to 2.40. With this material the complete photodegradation of a 0.20 mM phenol solution was achieved within 90 min, which is considerably faster when compared with the use of TiO_2. The occurrence of main degradation byproducts was also investigated.

1. Introduction

The treatment of industrial wastewaters for removing organic pollutants is nowadays a very important aspect of environmental technology. Consequently a growing interest in heterogeneous photocatalysis, as an advanced oxidation technique, has been developed [1,2]. The use of nanocrystalline semiconductors as photocatalysts, to initiate interfacial redox reactions, have generated great interest, due to their unique physicochemical properties, caused by their nanosized dimensions and large surface/volume ratios.

In this context, TiO_2 has been investigated as the most promising photocatalyst for the treatment of pollutants, from water and air, since it has a reasonable photoactivity under ultraviolet light irradiation (anatase, Eg = 3.2 eV), is not toxic, water insoluble, and comparatively inexpensive. However the two major limitations for its wide practical application are the small percentage of photons of the solar radiation, which has the required energy to photogenerate electrons and holes, and their high charge recombination rate. Another practical limitation is the photocatalyst removal; this problem can be overcome by the use of supported or sub-micrometric particles.

As a result, the development of visible light responsive-based TiO_2 photocatalyst, coupled with visible light sensitizers is an important goal to achieve in this active research area. Metals [3], non-metallic elements [4], dyes [5] or a second semiconducting nanophase [6] have been used as sensitizers. Simultaneously, and for the nanoscale coupled semiconductors, it can be expected that the TiO_2 photocatalytic activity will be significantly improved by the enhancement of charge separation and minimization or inhibition of charge–carrier recombination [7,8].

Several methods have been reported concerning the photosensitization of TiO_2 by M_xS_y or M_xO_y nanoparticles for heterogeneous photocatalysis [9], including CdS [10,11], Bi_2S_3 [11], WO_3 [12] or ZnS [13]. In this context, nanocrystalline Ag_2S is a good candidate for the photosensitization of TiO_2 catalysts. Indeed, Ag_2S has a direct band gap of 0.9–1.05 eV, its conduction band (−0.3 eV) is less anodic than the corresponding TiO_2 band (−0.1 eV) and the valence band (+0.7 eV) is more cathodic than the TiO_2 valence band (+3.1 eV) [8,9].

On the basis of these considerations, in this work it is reported for the first time, a study concerning the use of TiO_2/Ag_2S nanocomposites, as photocatalysts in the phenol photodegradation, under UV–vis radiation. The synthesis of the nanocomposites was achieved by a previously reported solution deposition method [14,15], making use of silver (I) diethyldithiocarbamate as a single-source for the Ag_2S, and of TiO_2 particles as growth substrates. Phenol was used as a model organic pollutant, due to the negative impact of its presence on several industrial wastewaters.

* Corresponding author. Tel.: +351 217500000; fax: +351 217500088.
E-mail address: ocmonteiro@fc.ul.pt (O.C. Monteiro).

1010-6030/$ – see front matter © 2009 Elsevier B.V. All rights reserved.
doi:10.1016/j.jphotochem.2009.03.014

2. Experimental

All reagents were of analytical grade (Aldrich and Fluka) and were used as received. The solutions were prepared with Millipore Milli-Q ultra pure water.

2.1. Materials synthesis

2.1.1. Ag_2S precursor [$Ag(S_2CN(C_2H_5)_2)$]

The metal dithiocarbamate complex was prepared by the reaction of 13.5 mmol of $Na[S_2CN(CH_2CH_3)_2]$ with 10 mmol of $AgNO_3$ in water (100 mL) [15]. The obtained solid was isolated by filtration and washed with water. The purity of the metal complex was checked by IR and ^1H NMR spectroscopies.

2.1.2. TiO_2 preparation

Nearly monodisperse spherical TiO_2 (anatase) particles were prepared by the controlled hydrolysis of titanium tetraethoxide in ethanol as described by Maret and co-workers [16]. Thus 100 mL of ethanol was mixed with 0.4 mL of an aqueous solution of KCl 0.1 M, followed by addition of 1.7 mL of $Ti(OC_2H_5)_4$, at room temperature under magnetic stirring. The reaction ran over 8 h, yielding in the end a colourless colloid. The solid was collected on a millipore membrane (0.25 μm) and then thoroughly washed with ethanol/water. The crystalline phase anatase-TiO_2 was obtained by thermal treatment at 500 °C, during 4 h.

2.1.3. TiO_2/Ag_2S nanocomposite synthesis

The nanocomposite particles were prepared as previously reported [14,15], by adding drop-wise ethylenediamine (2.5 mL) to an acetone solution (25 mL) containing 0.125 mmol of the Ag_2S precursor (Section 2.1.1) and 0.125 g of the TiO_2 particles previously prepared (Section 2.1.2). The suspension formed was then refluxed with stirring. The grey solids were collected for distinct reaction times and isolated by centrifugation and finally washed thoroughly with acetone. All the obtained powders were dried at room temperature in a dessicator containing silica gel. Distinct materials have been prepared for different reaction times, 1.5, 3, 5 and 7 h. For sake of clarity the nanocomposite samples were identified as TiO_2/Ag_2S (reaction time).

For comparative proposes TiO_2 P-25 from Degussa was also used for the nanocomposites preparation.

2.2. Photodegradation experiments

The photodegradation experiments have been conducted using an Ace Glass refrigerated photoreactor [17]. The reaction vessel (250 mL) was made of borosilicate glass and suitable to accommodate an immersion well. The quartz immersion well, was a double-walled, with inlet and outlet tubes for cooling. The inlet tube extends down the annular space and ensures the upward flow of coolant from the bottom of the well upward to the outlet. The reactor had one angled joint for the sparger tube, one vertical joint for the condenser and one Ace-Thread side arm for the thermometer. The reactor bottom is flat to allow the use of a magnetic stirrer. The radiation source was a 450-W medium-pressure mercury-vapour lamp (from Hanovia). Of the total radiated energy, approximately 40–48% is in the ultraviolet portion of the spectrum and 40–43% in the visible.

Suspensions have been prepared by adding 50 mg of the nanocomposite powder into a 100 mL of 0.2 mM phenol aqueous solution (0.05%, w/w), at pH 7. Prior to irradiation, the suspensions were stirred in dark conditions for 15 min. During irradiation, the suspensions were sampled, at regular intervals, centrifuged and analysed by UV–vis spectroscopy and high performance liquid chromatography (HPLC).

2.3. Characterization

X-ray powder diffraction was performed using a Philips X-ray diffractometer (PW 1730) with automatic data acquisition (APD Philips v3.6B) using Cu Kα radiation (λ = 0.15406 nm) and working at 40 kV/30 mA. The diffraction patterns were collected in the range $2\theta = 20–60°$ with a 0.01° step size and an acquisition time of 2.5 s/step. A UV–vis spectrophotometer Jasco V560 was used for monitoring the absorption of the phenolic solutions and the diffuse reflectance spectra (DRS) of the powders, in the range 200–900 nm at a scanning speed of 400 nm/min. The scanning electron microscope (SEM) images and energy-dispersive X-ray spectroscopy analysis (EDS) were carried out on a JEOL (JSM-35C) system operating at 15 keV. The X-ray photoelectron spectroscopy (XPS) spectra were taken in CAE mode (30 eV), using an Al (non-monochromate) anode. The accelerating voltage was 15 kV. The XPS spectra were taken in CAE mode (30 eV), using an Al (non-monochromate) anode. The accelerating voltage was 15 kV. The quantitative XPS analysis was performed using the Avantage software. The relative atomic concentration (A_x) was calculated using the following relation:

$$A_x = \frac{\text{normalised peak area}}{S_i \text{ normalised peak areas}} \times 100$$

where the subscript (x) refers to the quantified specie and the subscript (i) refers to the other species detected in the XPS spectra. The normalised peak area was obtained by dividing the intensity of the XPS peak of the species (after background subtraction) by the sensitivity factor of the corresponding specie. The background subtraction was performed using the Shirley algorithm, which gives a curve S shaped and assumes that the intensity of the background is proportional to the peak area on the higher kinetic energy side of the spectrum. The quantification was performed after peak fit. The peak fit function used was a Gaussian–Lorentzian product function and the algorithm was based on the Simplex optimisation as used in the Avantage software. The atomic absorption spectroscopy (AAS) analyses were performed in a Pye Unicam spectrometer. HPLC analysis were carried out on an Agilent 1100 Series LC chromatographic system (Agilent Technologies, Waldbronn, Germany) equipped with the following devices: vacuum degasser, quaternary pump, autosampler, thermostated column compartment and a diode array detector (DAD). Data acquisition was performed with the software LC3D ChemStation (version A.08.03; Agilent Technologies). A Tracer Excel 120 octadecilsilica-A, 150 mm × 4.0 mm column, with 5 μm particle size from Teknokroma (Spain) was used. The injection volume was 20 μL with a draw speed of 200 μL/min. The analysis was performed at 25 °C in isocratic conditions with a flow of 1 mL/min, using a mobile phase consisting of a mixture of 50% of methanol and 50% of an aqueous solution of 0.1% phosphoric acid. Phenol peak areas from the aqueous solutions of photodegradation assays were compared with pure standard controls.

3. Results and discussion

3.1. Material characterization

The TiO_2/Ag_2S nanocomposites were obtained by the reaction of the silver diethyldithiocarbamate complex with ethylenediamine in the presence of TiO_2 particles, for distinct reaction times. The nanocomposite materials were characterized by SEM, XRD, XPS and DRS. The composite powders were analysed by XRD (Fig. 1) and the TiO_2 *anatase* and Ag_2S *acanthite* were the crystalline phases identified. EDS shows the existence of Ag and S peaks in all the samples. However, for the TiO_2/Ag_2S(1.5 h) material, the confirmation of the crystalline Ag_2S phase, over the TiO_2 surface was inconclusive. This result suggests the presence of no-crystalline intermediate decomposition compounds over the TiO_2 surface, due to the reduced

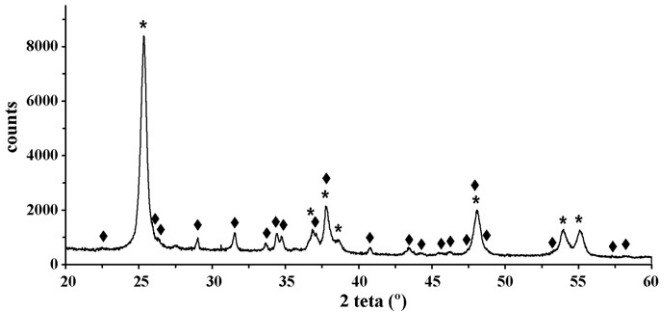

Fig. 1. XRD pattern of the TiO_2/Ag_2S(3 h) nanocomposite material (*: TiO_2 *anatase* and ♦: Ag_2S *acanthite*).

synthesis time. This fact was corroborated by the extremely pale colour of this solid when compared with the samples obtained for longer times (3, 5 and 7 h).

The SEM images of the TiO_2/Ag_2S nanocomposites, for different reaction times are shown in Fig. 2. The TiO_2 surface morphology, after 1.5 h of reaction, was identical to the original TiO_2 (not shown). The presence of small Ag_2S islands at the TiO_2 surface was visualized after 3 h of reaction time. By increasing the preparation time (7 h), an increase on the TiO_2 surface covering rate, with a simultaneous Ag_2S segregation occurrence, were observed. The XPS analysis of the grey solid, TiO_2/Ag_2S(3 h), was in agreement with the

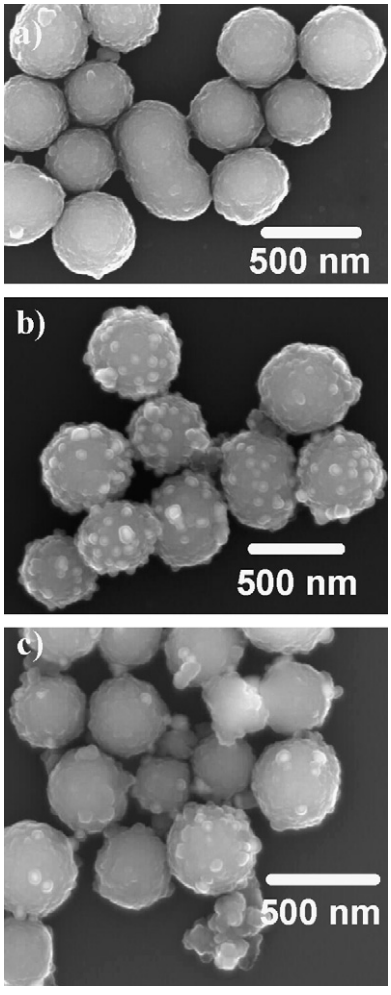

Fig. 2. SEM images of the nanocomposite TiO_2/Ag_2S prepared during (a) 1.5 h, (b) 3 h and (c) 7 h.

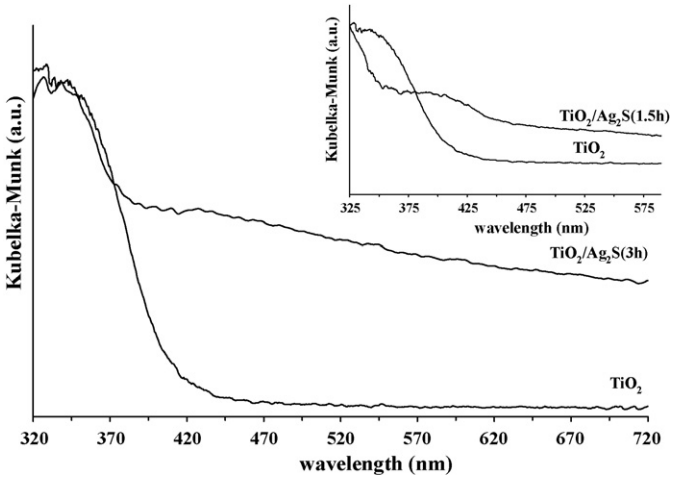

Fig. 3. Diffuse reflectance spectra of TiO_2/Ag_2S(3 h) and TiO_2 materials. Inset: Diffuse reflectance spectra of TiO_2 and TiO_2/Ag_2S(1.5 h).

presence of a Ag_2S phase over the TiO_2 surface. A surface atomic ratio Ti/Ag equal to 2.40 was obtained for this nanocomposite.

In order to check the visible photo-response of the TiO_2/Ag_2S(3 h) and TiO_2 materials, their diffuse reflectance spectra (DRS) were measured. As shows in Fig. 3 the TiO_2/Ag_2S(3 h) material reflects less radiation on the visible range than TiO_2 alone. This fact is related with the Ag_2S presence, a semiconductor with a direct band gap of 0.9–1.05 eV, over the TiO_2 surface and is in agreement with the results obtained by Weller and Hoyer [18]. This result opens the possibility of using this nanocomposite material as a photocatalyst on degradation processes with lower energetic requirements when compared with TiO_2. Fig. 3, inset shows the diffuse reflectance spectra of the TiO_2 particles and the same particles after 1.5 h of synthesis. As can be observed, the DRS of TiO_2/Ag_2S(3 h) did not present the characteristic TiO_2 absorption band (at 425 nm) and only a slight increase on the absorption at 450 and 350 nm was visualized. This result is in agreement with a material presenting no absorption properties, on the visible range. In these conditions the TiO_2 is probably covered by a shell material that inhibits completely the absorption of the core.

3.2. Phenol photodegradation

On a photocatalytic process, the adsorption characteristics of the photocatalyst/pollutant system are considered important parameters, since the photo-oxidation usually takes place at the catalyst surface.

The TiO_2 and TiO_2/Ag_2S ability to adsorb phenol was investigated in the absence of light. As reported by others [19], no experimental evidence of the phenol adsorption was observed.

3.2.1. UV–vis analysis

Aiming to select the best photocatalyst for the phenol photodegradation process, preliminary experiments were performed by monitoring the phenol degradation reaction by UV–vis spectroscopy [20–22]. The phenol photodegradation in the absence of catalyst (photolysis) was also evaluated. The solution absorbance at 270 nm, typical phenol maximum absorption peak, was used as reference for the photodegradation analysis.

Fig. 4 shows the absorption spectra of a 0.2 mM phenol solution, after 120 min of irradiation, in the presence of distinct TiO_2/Ag_2S nanocomposites. The absorbance at 270 nm of the initial solution (0.2 mM phenol), is shown for comparison purposes.

The best catalytic activity, concerning the phenol photodegradation, was obtained using the TiO_2/Ag_2S(3 h) nanocomposite. It

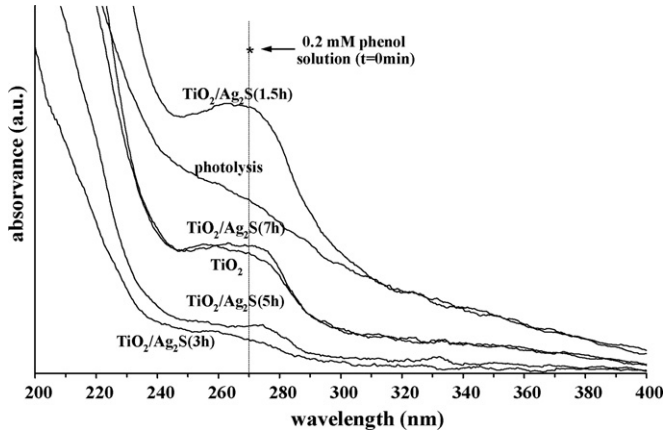

Fig. 4. Absorption spectra of a phenol solution (0.2 mM) after 120 min of photodegradation using 0.50 g/L of different photocatalysts (optical path length = 1 cm).

can be seen (Fig. 4), that after 120 min of irradiation no peaks related with the phenolic compounds appear on its absorption spectrum. On the contrary, using the same experimental conditions, TiO_2/Ag_2S(1.5 h) exhibit the lowest photocatalytic activity of all the tested materials. This result can be explained by two main reasons. First, the DRS of the solid TiO_2/Ag_2S(1.5 h) shows a blue shift on the absorption energy onset (from 425 to 350 nm) and a simultaneous decrease on the total absorbed energy when compared with the TiO_2 (Fig. 3, inset). In these circumstances the TiO_2 photoactivity was drastically reduced. In addition when a high particles concentration (with no catalytic properties) is used the suspensions turbidity increases. In this situation the light penetration decreases, as a result of an enhanced light scattering effect, and consequently the photodegradation will be less effective [23,24].

On the other hand it is interesting to observe that the phenol absorption peak increases with increasing TiO_2/Ag_2S reaction time (3, 5 and 7 h). This result suggests that an increase of Ag_2S over the TiO_2 surface, and therefore a consequent decrease of the solutes access to the surface, can be directly linked with the photocatalytic activity of the TiO_2.

Concerning the above results, the phenol photodegradation was performed in the presence of TiO_2/Ag_2S(3 h). Fig. 5 shows the spectra of a 0.2 mM phenol aqueous solution, for different irradiation times, in the presence of TiO_2/Ag_2S(3 h). A clear decrease on the 270 nm absorbance peak, characteristic of the phenol existence

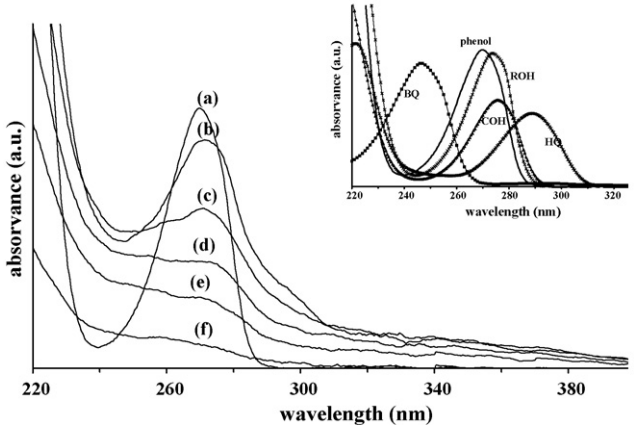

Fig. 5. Absorption spectra of a phenol solution (0.2 mM) for distinct photodegradation times: *t* = (a) 0 min, (b) 30 min, (c) 60 min, (d) 75 min, (e) 90 min and (f) 120 min, using 0.50 g/L of TiO_2/Ag_2S(3 h) as photocatalyst. Inset: Absorption spectra of phenol, hydroquinone (HQ), benzoquinone (BQ), resorcinol (ROH) and catechol (COH) aqueous solutions (optical path length = 1 cm).

[25], was observed with the increase on the irradiation time. Similar spectra behaviour has been obtained for all the materials tested, including TiO_2. These spectra are considerably different from the ones recorded during the photolysis process, where a considerable increase on the 270 nm absorbance peak was observed, for the initial times of photo-irradiation. This previous observation has been reported by others researchers [22], and has been attributed to an initial and very fast formation of phenol photodegradation main byproducts (e.g. catechol, resorcinol, hydroquinone and benzoquinone) which absorbs on the same wavelength region of phenol. Regarding these facts, one can predict the existence of a pathway for the TiO_2/Ag_2S catalysed phenol photodegradation, that is different of the photolysis process.

A more detailed analysis of Fig. 5 shows, for the initial times of irradiation, a slight decrease and enlargement on the 270 nm absorbance peak. A simultaneous increase on the 245 and 288 nm absorbance peaks was also observed. The enlargement of the 270 nm absorbance peak can be associated with the presence of both catechol and resorcinol, with maximum absorption peaks at 275 and 273 nm respectively (Fig. 5, inset). On the other hand the increase of the absorbance at 245 and 288 nm can be attributed to the presence of benzoquinone, which absorbs at 246 nm, and hydroquinone which has the maximum absorption peak at 288 nm (Fig. 5, inset).

A comparative analysis of the photocatalytic performances of TiO_2 and TiO_2/Ag_2S(3 h) concerning the phenol degradation reveals, for both materials, a continuous decrease on the phenolic compounds, during the 120 min of photo-irradiation (Fig. 6, curves a and b). Considering these experimental results, one can say that phenol photocatalytic degradation is faster using TiO_2/Ag_2S(3 h) than TiO_2. The enhancement of the TiO_2 visible light absorption, consequence of the photosensitization, associated with an electron trapping phenomena by the nanocrystalline Ag_2S is the most probable mechanism to explain these results.

For comparative proposes, TiO_2(P-25), from Degussa, and a TiO_2(P-25)/Ag_2S(3 h) samples were also tested for the phenol photodegradation. Although this was not the main goal of this work it is possible to conclude that, under identical experimental conditions, the TiO_2(P-25) was a better photocatalyst for the phenol photodegradation compared with the TiO_2 and TiO_2/Ag_2S(3 h) prepared samples. However, the photosensitized TiO_2 (P-25) with Ag_2S, the TiO_2 (P-25)/Ag_2S(3 h) was the material presenting the best photocatalytic activity from all the materials tested. This result allows us to conclude that the TiO_2 photosensitization process, independently of the type of TiO_2 used leads to a material with enhanced photocatalytic performance.

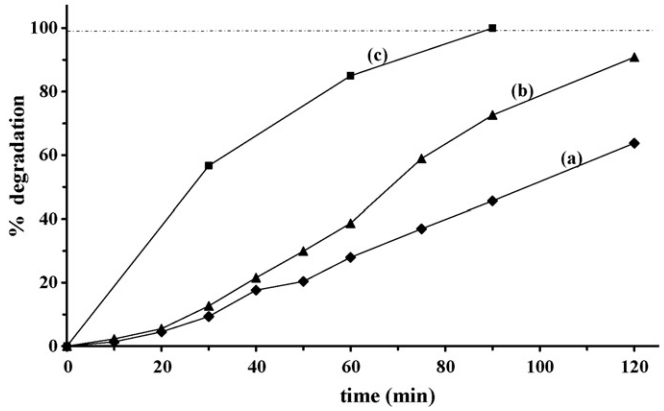

Fig. 6. Phenolic compounds degradation (%) (by UV–vis analysis), using TiO_2 (a) and TiO_2/Ag_2S(3 h) (b) as photocatalyst. Phenol degradation (%) using TiO_2/Ag_2S(3 h) as photocatalyst (c) obtained by HPLC-DAD analysis.

In addition, the UV–vis spectra of the irradiated solutions, using TiO_2 (P-25) (supplementary material—Fig. 8) and TiO_2(P-25)/Ag_2S(3 h) as photocatalysts, were similar but different from the ones obtained using TiO_2 and TiO_2/Ag_2S(3 h) (Fig. 5). The hydroquinone/benzoquinone ratio seems to be higher when the Degussa materials were used. This fact suggests a different mechanism for the phenol photodegradation process.

In face of these preliminary results, additional work must be done in order to understand the mechanistic differences between theses catalysts and to decide which is the best photocatalyst.

3.2.2. Phenol byproducts identification

In order to identify and quantify the phenolic compounds during the phenol photocatalytic degradation process HPLC measurements from the reaction solutions, have been performed. The HPLC data obtained during the phenol photodegradation in the presence of TiO_2/Ag_2S(3 h), shows the complete phenol disappearance after 90 min of irradiation (Fig. 6, curve c). After this time, only phenol degradation byproducts were present in solution, and were subject of photodegradation.

The main intermediates in phenol photocatalytic degradation process have been experimentally identified by other authors [26,27] as hydroquinone, catechol, benzoquinone and resorcinol, depending on the mechanism. In the present work, the identification of the phenol photodegradation intermediates, after 30, 60 and 90 min of photo-irradiation in the presence of TiO_2/Ag_2S(3 h) has been performed by HPLC. The results show that the major intermediates were catechol and benzoquinone with the highest concentration level after 30 min of irradiation. After 120 min, the HPLC analyses showed the existence of vestigial quantities of these compounds (catechol and benzoquinone) in solution. The presence of hydroquinone and resorcinol has not been detected for the samples analysed. These results are in agreement with the previous ones obtained by the UV–vis spectra qualitative analysis, for the phenolic compounds photodegradation.

3.2.3. Photocatalyst stability

In order to check the photochemical stability of the TiO_2/Ag_2S(3 h) nanocomposite the solid and the solution have been analysed after being submitted to photo-irradiation. Due to the ability of silver ions to be reduced and adsorbed on the TiO_2 surface, the XRD of the solid, after being used on the photodegradation process, was performed. The XRD patterns (see supplementary material) only show the existence of the TiO_2 and Ag_2S crystalline phases with a slight change on the peaks intensity. A slight red shift on the photocatalyst band gap, after photo-irradiation, was also observed. These results may be related with a small increase on the crystallite dimensions due to a possible photo-irradiation activation process. The Ag_2S photo-stability was also confirmed by AAS. No traces of Ag have been detected in solution.

Considering the good results obtained for the use of TiO_2, after photosensitization with Ag_2S, on the phenol photodegradation process, under UV–vis radiation, it is possible to propose these materials as potential phenol photocatalysts under solar light irradiation. Concurrently the photocatalytic degradation of others pollutants, using these materials are now in progress in our laboratory.

4. Conclusions

In this work the photosensitization of TiO_2 with Ag_2S, by a chemical deposition method, has been performed. The photocatalytic behaviour of the obtained materials was investigated, for the first time, on a pollutant degradation process. The TiO_2/Ag_2S nanocomposite materials have shown better phenol photocatalytic activity than TiO_2. In the conditions of our experiments the best phenol photocatalyst was TiO_2/Ag_2S with a Ti/Ag atomic ratio equal to 2.40. The complete photodegradation of a 0.2 mM phenol solution was achieved, using 0.05% (w/w) of this nanocomposite material, in 90 min. The evaluation of the main phenol degradation byproducts was also carried out.

Acknowledgments

O.C. Monteiro thank Fundação para a Ciência e Tecnologia (FCT) for the grant SFRH/BPD/14554/2003. Márcia C. Neves thank the University of Aveiro for a PhD grant. This work is supported by FCT, POCI and co-financed by FEDER (PPCDT/QUI/59615/2004).

Appendix A. Supplementary data

Supplementary data associated with this article can be found, in the online version, at doi:10.1016/j.jphotochem.2009.03.014.

References

[1] D. Chatterjee, S. Dasgupta, Visible light induced photocatalytic degradation of organic pollutants, J. Photochem. Photobiol. C 6 (2005) 186–205.
[2] V. Augugliaro, M. Litter, L. Palmisano, J. Soria, The combination of heterogeneous photocatalysis with chemical and physical operations: a tool for improving the photoprocess performance, J. Photochem. Photobiol. C 7 (2006) 127–144.
[3] D.H. Kim, D. Choi, S. Kim, K.S. Lee, The effect of phase type on photocatalytic activity in transition metal doped TiO_2 nanoparticles, Catal. Commun. 9 (2008) 654–657.
[4] J. Yang, H. Bai, Q. Jiang, J. Lian, Visible-light photocatalysis in nitrogen–carbon-doped TiO_2 films obtained by heating TiO_2 gel-film in an ionized N_2 gas, Thin Solid Films 516 (2008) 1736–1742.
[5] D. Jiang, Y. Xu, B. Hou, D. Wu, Y. Sun, Synthesis of visible light-activated TiO_2 photocatalyst via surface organic modification, J. Solid State Chem. 180 (2007) 1787–1791.
[6] R. Brahimi, Y. Bessekhouad, A. Bouguelia, M. Trari, Improvement of eosin visible light degradation using PbS-sensititized TiO_2, J. Photochem. Photobiol. A 194 (2008) 173–180.
[7] R. Vogel, P. Hoyer, H. Weller, Quantum-sized PbS, CdS, Ag_2S, Sb_2S_3 particles as sensitizers for various nanoporous wide-bandgap semiconductors, J. Phys. Chem. 98 (1994) 3183–3188.
[8] A.I. Kryukov, S.Y. Kuehmii, V.D. Pokhodenko, Energetics of electron processes in semiconductor photocatalytic systems, Theor. Exp. Chem. 36 (2000) 63–81.
[9] D. Robert, Photosensitization of TiO_2 by M_xO_y and M_xS_y nanoparticles for heterogeneous photocatalysis applications, Catal. Today 122 (2007) 20–26.
[10] J.C. Kim, J. Choi, Y.B. Lee, J.H. Hong, J.I. Lee, J.W. Yang, W.I. Lee, N.H. Hur, Enhanced photocatalytic activity in composites of TiO_2 nanotubes and CdS nanoparticles, Chem. Commun. (2006) 5024–5026.
[11] Y. Bessekhouad, D. Robert, J.V. Weber, Bi_2S_3/TiO_2 and CdS/TiO_2 heterojunctions as an available configuration for photocatalytic degradation of organic pollutant, J. Photochem. Photobiol. A 163 (2004) 569–580.
[12] V. Puddu, R. Mokaya, G.L. Puma, Novel one step hydrothermal synthesis of TiO_2/WO_3 nanocomposites with enhanced photocatalytic activity, Chem. Commun. (2007) 4749–4751.
[13] V. Stengl, S. Bakardjieva, N. Murafa, V. Houšková, K. Lang, Visible-light photocatalytic activity of TiO_2/ZnS nanocomposites prepared by homogeneous hydrolysis, Micropor. Mesopor. Mater. 110 (2008) 370–378.
[14] O.C. Monteiro, M.C. Neves, T. Trindade, Zinc sulfide nanocoating of silica submicron spheres using a single-source method, J. Nanosci. Nanotechnol. 4 (2004) 137–142.
[15] M.C. Neves, O.C. Monteiro, R. Hempelmann, A.M.S. Silva, T. Trindade, From single-molecule precursors to Ag_2S/TiO_2 nanocomposites, Eur. J. Inorg. Chem. (2008) 4380–4386.
[16] S. Eiden-Assmann, J. Widoniak, G. Maret, Synthesis and characterization of porous and nonporous mondisperse colloidal TiO_2 particles, Chem. Mater. 16 (2004) 6–11.
[17] A. Franco, M.C. Neves, M.M.L. Ribeiro Carrott, M.H. Mendonça, M.I. Pereira, O.C. Monteiro, Photocatalytic decolorization of methylene blue in the presence of TiO_2/ZnS nanocomposites, J. Hazard. Mater. 161 (2009) 545–550.
[18] P. Hoyer, H. Weller, Particle size and pH effects on the sensitization of nanoporous titanium dioxide electrodes by Q-sized silver sulphide, Chem. Phys. Lett. 224 (1994) 75–80.
[19] C. Chiou, C. Wu, R. Juang, Influence of operating parameters on photocatalytic degradation of phenol in UV/TiO_2 process, Chem. Eng. J. 139 (2008) 322–329.

[20] S. Liu, X. Chen, A visible light response TiO_2 photocatalyst realized by cationic S-doping and its application for phenol degradation, J. Hazard. Mater. 152 (2008) 48–55.
[21] B. Roig, C. Gonzalez, O. Thomas, Monitoring of phenol photodegradation by ultraviolet Spectroscopy, Spectrochim. Acta, Part A 59 (2003) 303–307.
[22] G. Colón, M.C. Hidalgo, J.A. Navío, E. Melián, O.G. Díaz, J.M. Doña, Influence of amine template on the photoactivity of TiO_2 nanoparticles obtained by hydrothermal treatment, Appl. Catal. B 78 (2008) 176–182.
[23] E. Bizani, K. Fytianos, I. Poulios, V. Tsiridis, Photocatalytic decolorization and degradation of dye solutions and wastewaters in the presence of titanium dioxide, J. Hazard. Mater. 136 (2006) 85–94.
[24] S. Senthilkumaar, K. Porkodi, Heterogeneous photocatalytic decomposition of Crystal Violet in UV-illuminated sol–gel derived nanocrystalline TiO_2 suspensions, J. Colloid Interface Sci. 288 (2005) 184–189.
[25] I.B. Berlman, Handbook of Fluorescence Spectra of Aromatic Molecules, 2nd ed., Academic Press, New York, 1971.
[26] Y. Ao, J. Xu, D. Fu, X. Shen, C. Yuan, Low temperature preparation of anatase TiO_2-coated activated carbon, Colloids Surf. A 312 (2008) 125–130.
[27] A. Sobczynski, L. Duczmal, W. Zmudzinski, Phenol destruction by photocatalysis on TiO_2: an attempt to solve the reaction mechanism, J. Mol. Catal. A: Chem. 213 (2004) 225–230.